energies

MDPI

Article

A Modified Geometry-Based MIMO Channel Model for Tunnel Scattering Communication Environments

Denghong Tang [1,*], Xiaoli Xi [1,*] and Qianying Fan [2]

[1] Institute of Advanced Navigation and Electromagnetics, Xi'an University of Technology, Xi'an 710048, China
[2] Meteorological Bureau of Shanxi Province, Xi'an 710014, China; fanqianying1@163.com
* Correspondence: tang@stu.xaut.edu.cn (D.T.); xiaolixi@xaut.edu.cn (X.X.); Tel.: +86-1862-646-5105 (D.T.)

Abstract: In this study, a modified non-stationary geometry-based scattering model for tunnel vehicle-to-vehicle (V2V) multiple-input multiple-output Ricean fading channels is presented. The proposed channel introduces non-line-of-sight three-dimensional multi-bounced scattering propagation paths under an assumption of equivalent scattering points to depict the tunnel environments, in which the scatterers are randomly distributed on the semi-cylindrical tunnel wall (i.e., cable racks, jetfans, road signs, lighting facilities). Furthermore, the time-varying channel statistics (i.e., the space and frequency correlation functions) resulting from the relative movement between the mobile transmitter and mobile receiver are analyzed. Finally, numerical results show that the space correlations of the proposed model significantly decrease when the multi-bounced scattering rays are taken into account; moreover, when the velocity and the antenna angle γ_R increase, the correlations decrease therewith, which exhibits good agreement with the existing V2V scattering channel models and measured data in a real tunnel environment, demonstrating the rationality of the underlying channel model.

Keywords: tunnel wireless communications; multi-bounced scattering; time-varying correlation functions; geometry-based models

Citation: Tang, D.; Xi, X.; Fan, Q. A Modified Geometry-Based MIMO Channel Model for Tunnel Scattering Communication Environments. *Energies* **2022**, *15*, 5120. https://doi.org/10.3390/en15145120

Academic Editors: Hongming Zhang and Hao Jiang

Received: 10 June 2022
Accepted: 13 July 2022
Published: 14 July 2022

1. Introduction

Vehicle-to-vehicle (V2V) communication has recently attracted great attention regarding new traffic telematic applications, which can improve safety and mobility on roads. To achieve the best performance of future V2V communication systems in tunnel multiple-input multiple-output (MIMO) environments, it is essential to have detailed knowledge of the statistical properties of the underlying radio channel [1].

In general, wireless channel modeling has been an important research topic in tunnel V2V communication environments [2–6]. Arshad et al. [2] proposed a ray tracing method to simulate the propagation of signals in a curved tunnel environment, and further explored the impact of the layout of tunnel base stations on signal coverage. However, this method has high computational complexity and includes some unrealistic approximations. In 2014, Forooshani et al. [3] introduced a multi-mode wave-guide model to predict the phenomenon of signal angular dispersion in tunnel environments, and proved that the wave-guide model can be used to model the signal transmission in far-field regions of tunnels, though not in the case of multi-mode coexistence in near-field regions. Overall, the V2V channel models in the above tunnel scenarios belong to deterministic modeling, where the influences of spatial distributions of various potential scatterers on the statistical characteristics of wireless fading channels are not considered. Therefore, Avazov and Pätzold [4] adopted a geometrical wideband MIMO V2V scattering stochastic channel model to analyze the correlation characteristics of the line-of-sight (LoS) and non-LoS (NLoS) propagation signals in semi-circular tunnel environments. Furthermore, Zhang et al. [5] presented a propagation graph theory-based wireless channel modeling method for NLoS tunnel scenarios, in which the impact of tunnel bending angles on the wideband channel characteristics was verified.

However, the multi-bounced propagation paths between the mobile transmitter (MT) and mobile receiver (MR) are ignored in most previous models. It is reported in [6] that the density of receiving signal links in three-dimensional (3D) dynamic dense tunnel environments would significantly increase for next-generation communications. Therefore, the single-bounced assumption in channel modeling is rather restrictive due to the large amount of potential scatterers. Subsequently, Pätzold et al. [7] proposed an adaptive geometry-based stochastic model to describe wideband V2V fading channels in T-junction communication environments, in which they focused on the single- and double-bounced conditions. Nevertheless, the angular extension of scattering rays in 3D space was not discussed. In [8], He et al. explored the channel characteristics of tunnel communication scenarios for both straight and curved routes on the basis of a ray tracer calibrated with measurements taken in a Seoul subway line, where scatterers are fixed at the side wall and pylons of the rectangular tunnel to model the key time-variant channel parameters and their correlations. However, they neglected the impacts of the tunnel top wall scattering on the V2V channel statistics. Meanwhile, the uncertainty of scattering numbers in the above two models were not considered. On the other hand, Tang et al. [9] presented a multi-bounced scattering MIMO channel model for tunnel LoS and NLoS propagation rays based on the ellipse-based single-bounce model, where the closed angle-of-departure (AOD) and angle-of-arrival (AOA) characteristics were analyzed. However, most previous channel models do not take into account the effects of the moving properties on channel statistics.

Here, we present a modified non-stationary geometry-based scattering tunnel V2V MIMO channel model, as illustrated in Figure 1. The main contributions of this study are as follows. (1) To the best of our knowledge, this is the first geometrical stochastic tunnel scattering model that considers multi-bounced scattering propagation paths. The assumption of equivalent scattering points and the statistical distributions of effective scatterers are designed according to the actual tunnels; thus, the model is suitable for describing real tunnel V2V scenarios. (2) The space correlation functions (CFs) of the proposed model are verified by comparing them with those from the existing scattering channel models and measurements in tunnel V2V wireless communication environments. (3) The impacts of the reflected numbers as well as the tunnel parameters and moving properties on the V2V channel statistics are investigated in detail, the results of which can be used for the design and performance evaluation of vehicular tunnel systems.

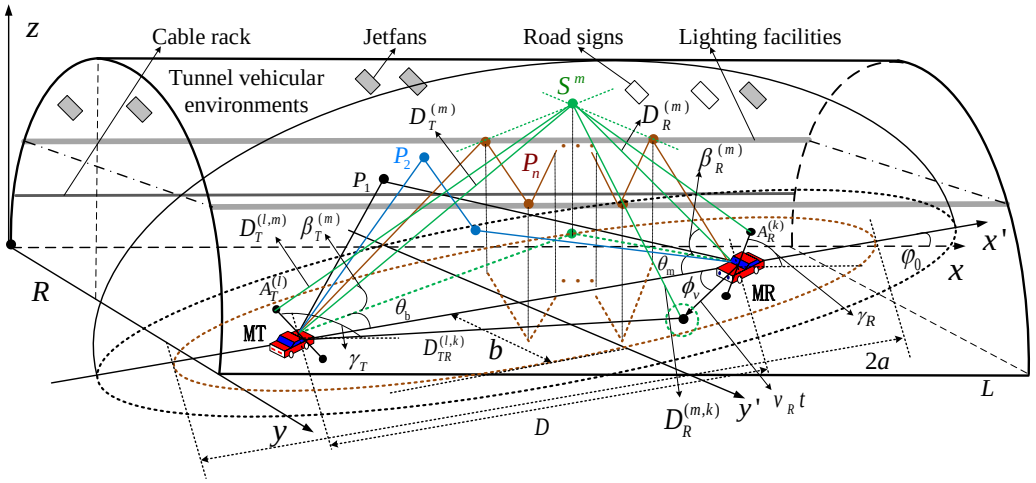

Figure 1. Proposed non-stationary geometry-based scattering channel model for tunnel V2V communication environments.

2. Proposed Geometry-Based Tunnel V2V Channel Model

2.1. Descriptions of the Proposed Model

Figure 1 shows the geometry of the proposed model with uniform linear-array transmitter and receiver antennas. The number of transmitter and receiver antenna array

elements are denoted as M_T and M_R, respectively. As shown in Figure 1, the length and section radius of the semi-circular tunnel are denoted as L and R, respectively. The original position of the center of the MT and MR are indicated by the coordinates $(x_T, y_T, 0)$ and $(x_R, y_R, 0)$, respectively. $D = \left[(x_R - x_T)^2 + (y_R - y_T)^2\right]^{1/2}$ represents the original distance between the MT and MR center. Additionally, the MR is supposed to move in a relative direction ϕ_v to the MT with a constant velocity of v_R at time instant t. In the proposed model, we assume that waves at the MR antenna include the LoS component from the MT and the NLoS rays reflected by scatterers in tunnel environments. Note that P_1 and P_2 denote the single-bounced and double-bounced scattering paths in NLoS rays, respectively, while P_n denotes the multi-bounced scattering path when the reflected number is $n(n = 1, 2, \ldots, N)$, where N denotes the maximum number of reflections considered.

The traditional geometry-based elliptical model has been proved to be suitable for outdoor microcell wireless propagation environments. Therefore, the NLoS scattering in tunnel conditions still follows the elliptical model, and most of the effective scatterers are densely distributed along the tunnel walls. To further characterize the proposed model, the multi-bounced scattering is approximately visualized to single-bounce elliptical scattering through the geometric transformation method in [9], where the equivalent scattering point of the multi-bounced scattering model is defined as $S^m(m = 1, 2, \ldots, M)$, as shown in Figure 1. However, since we take into account the consideration of the angular extension in the elevation plane, the proposed equivalent scattering model consequently presents a semi-ellipsoid shape. Moreover, the horizontal projection of each equivalent scattering path corresponds to a traditional elliptical single-scattering model. It can be observed that the ellipse shape will be tilted when the relative positions of the MT and MR and the reflected number change. Thus, we define the connection of MT and MR as the new coordinate axis x', and transform the coordinates (x, y, z) into (x', y', z') by the rotation angle $\varphi_0 = \arctan\left(\frac{2R - 2y_R}{x_R - x_T}\right)$. In this case, the generalized equation of the proposed tunnel equivalent ellipsoidal model can be expressed as

$$\frac{(2x - y_R \cot\varphi_0)^2(\cos\varphi_0 - \sin\varphi_0)^2}{4a^2} + \frac{(2y - y_R)^2(\cos\varphi_0 + \sin\varphi_0)^2}{4b^2} + \frac{z^2}{R^2} = 1, \quad (1)$$

with the semi-major and semi-minor dimensions of the ellipse being, respectively, denoted as $a = (2nR - y_R)\csc\varphi$ and $b = nR - y_R$, where the n-related angle is represented as $\varphi = \arctan\left(\frac{4nR - 2y_R}{x_R - x_T}\right)$.

In the proposed model, the antenna element spacings at the MT and MR are denoted by δ_T and δ_R, respectively. The orientations of the transmitter and receiver antenna arrays are both perpendicular to the z-axis, while the angles relative to the x-axis are denoted as γ_T and γ_R, correspondingly. θ_b and θ_m denote the signal AOD and AOA in the azimuth plane, respectively. In addition, the LoS distance from the lth transmitter antenna element $A_T^{(l)}(l = 1, 2, \ldots, M_T)$ to the kth receiver antenna element $A_R^{(k)}(k = 1, 2, \ldots, M_R)$ is denoted as $D_{TR}^{(l,k)}$. Similarly, the AOD and AOA of the NLoS rays in the elevation plane are denoted as β_T^m and β_R^m, respectively. The NLoS distances from $A_T^{(l)}$ and $A_R^{(k)}$ to S^m are denoted as $D_T^{(l,m)}$ and $D_R^{(m,k)}$, respectively. The NLoS distances from the MT and MR center to S^m are denoted as $D_T^{(m)}$ and $D_R^{(m)}$, respectively. As mentioned in most prior work [10], the reference wideband MIMO V2V channel can be described by the complex channel matrix $\mathbf{H}(t) = [h_{lk}(t)]_{M_R \times M_T}$. Moreover, the complex channel response between $A_T^{(l)}$ and $A_R^{(k)}$ at the carrier wavelength λ can be expressed as

$$h_{lk}(t) = h_{lk}^{LOS}(t) + \sum_{i=1}^{N} h_{lk}^{NLOS}(t), \quad (2)$$

where

$$h_{lk}^{LOS}(t) = \sqrt{\frac{C_R}{C_R+1}} \times e^{j2\pi\left[f_{\max}\cos(\phi_v)t - D_{TR}^{(l,k)}/\lambda\right]} \tag{3}$$

$$h_{lk}^{NLOS}(t) = \sqrt{\frac{\eta_i}{(C_R+1)M}} \lim_{M\to\infty} \sum_{m=1}^{M} e^{-j2\pi\left(D_T^{(l,m)} + D_R^{(m,k)}\right)/\lambda} \times e^{j\left[2\pi f_{\max}\cos(\theta_m+\phi_v)t + \theta^{(m)}\right]}, \tag{4}$$

with C_R representing the Rice factor, which is defined as the ratio of the average power of the LoS component to that of the NLoS component. Furthermore, $f_{\max}$ denotes the maximum Doppler frequencies associated with the MR, and the energy-related parameter η_i specifies the reflected numbers of the NLoS scattering signals, which can be normalized as $\sum_{i=1}^{N} \eta_i = 1$. The symbol $\theta^{(m)}$ represents the phase shift caused by the interaction between the emitted waves and scatterers, which is assumed to be independent and identically distributed random variables with uniform distributions over $[0, 2\pi)$.

2.2. Multiple Propagation Channel Parameters

Many researchers have stated that the non-stationarity of future V2V channels, on account of the mobility between the MT and MR, is a significant feature compared with conventional cellular channels [11]. Consequently, the original fixed geometric path lengths are replaced by the time-varying channel statistics to capture the non-stationarity of the proposed vehicular tunnel channel. Since $\max\{\delta_T, \delta_R\}$ is far less than D, the LoS AoD and AoA are both approximately equal to 0 (i.e., $\theta_b = \theta_m = 0^\circ$). Then, the time-varying LoS distance $D_{TR}^{(l,k)}$ can be computed as

$$D_{TR}^{(l,k)}(t) = \sqrt{\left(D_0^{(l,k)}\right)^2 + (v_R t)^2 - 2D_0 v_R t\cos\phi_v}, \tag{5}$$

where

$$D_0^{(l,k)} = \Big[D^2 + (k_l\delta_T)^2 - 2Dk_l\delta_T\cos(\gamma_T - \varphi_0) + (k_k\delta_R)^2 + 2k_k\delta_R\cos(\gamma_R - \varphi_0) \times \sqrt{D^2 + (k_l\delta_T)^2 - 2Dk_l\delta_T\cos(\gamma_T - \varphi_0)}\Big]^{1/2} \tag{6}$$

with $k_l = (M_T - 2l + 1)/2$ and $k_k = (M_R - 2k + 1)/2$. On the other hand, the path lengths from the MT and MR center to the equivalent horizontal ellipse model are, respectively, designated as r_b and r_m. As mentioned in [9], they are geometrically calculated as

$$r_b = \frac{\left\{Db^2\cos\theta_b + \sqrt{D^2b^4\cos^2\theta_b - \left(b^2\cos^2\theta_b + a^2\sin^2\theta_b\right)\left(D^2b^2 - 4a^2b^2\right)}\right\}}{2\left(b^2\cos^2\theta_b + a^2\sin^2\theta_b\right)} \tag{7}$$

$$r_m = \sqrt{D^2 + r_b^2 - 2Dr_b\cos\theta_b} \tag{8}$$

Here, we take into account the impact of angular spreads in both the azimuth and elevation plane on the channel statistics; moreover, the AODs and AOAs of the NLoS rays in the proposed ellipsoidal scattering model are closely related. Thus, the closed-form expressions of the NLoS distances are supposed to be functions of the AODs θ_b and β_T^m, which can be derived as

$$D_T^{(l,m)} = \sqrt{{r_b}^2 + (k_l\delta_T)^2 - 2r_bk_l\delta_T\cos(\gamma_T - \varphi_0 - \theta_b) + \left(r_b\tan\beta_T^m\right)^2} \tag{9}$$

$$D_R^{(m,k)}(t) = \sqrt{\left(D_R^{(m)}\right)^2 + (v_R t)^2 - 2 r_m v_R t \cos(\theta_m + \phi_v) + \left(r_b \tan \beta_T^m\right)^2} \tag{10}$$

with $D_R^{(m)} = \sqrt{{r_m}^2 + (k_k \delta_R)^2 + 2 r_m k_k \delta_R \cos(\gamma_R - \varphi_0 + \theta_m)}$ and $\theta_m = \arcsin[(r_b \sin \theta_b)/r_m\,]$.

3. Statistical Properties of the Proposed Model

As mentioned in [12], the space CFs express the similarity between scattered multi-path fading signals, which can be used to specify the fading characteristic of wireless channels in terms of the time and movement. Therefore, the normalized time-variant space CFs between the complex channel responses $h_{lk}(t)$ and $h_{l'k'}(t+\tau)$ can be defined as

$$\rho_{lk,l'k'}(t,\tau) := \frac{E\left[h_{lk}^*(t) h_{l'k'}(t+\tau)\right]}{\sqrt{E\left[\left|h_{lk}(t)\right|^2\right] E\left[\left|h_{l'k'}(t+\tau)\right|^2\right]}} \tag{11}$$

where $(\,)^*$ is the complex conjugate operation and $E[\,]$ designates the statistical expectation operator. Furthermore, note that when the number of scatterers in the proposed model approaches infinity, i.e., $M \to \infty$, the discrete AODs θ_b and β_T^m can be replaced by continuous variables θ and β, respectively. Similarly, the NLoS distances and discrete CFs in Equation (9) can also be replaced with continuous functions. Here, the scatterers in the proposed ellipsoid scattering region are assumed to follow a uniform distribution. Therefore, by substituting Equations (3) and (4) into Equation (9), the time-variant space CFs for the LoS and NLoS paths can be, respectively, calculated as

$$\rho_{lk,l'k'}^{LOS}(t,\tau) = C_R e^{j2\pi\left[f_{\max}\cos(\phi_v)\tau - \left(D_{TR}^{(l,k)} - D_{TR}^{(l',k')}\right)/\lambda\right]} \tag{12}$$

$$\rho_{lk,l'k'}^{NLOS}(t,\tau) = \frac{3\eta_i}{2\pi R a b} \int_{-\pi}^{\pi} \int_{0}^{\pi/2} e^{j2\pi\tau f_{\max}\cos\{\arcsin[(r_b \sin\theta)/r_m\,] + \phi_v\}} \times e^{-j2\pi\left(D_T^{(l,m)} + D_R^{(m,k)} - D_T^{(l',m)} - D_R^{(m,k')}\right)/\lambda} d\beta d\theta \tag{13}$$

Obviously, the proposed space CFs depend not only on the proposed channel model parameters, but also on the non-stationary characteristics.

4. Numerical Results and Discussions

In this section, the statistical properties of the proposed non-stationary tunnel V2V channel model are evaluated and analyzed, where the antenna element spacings at the MT and MR are assumed to be equal [13–15]. Furthermore, the following parameters are set for our numerical analysis: $(x_T, y_T, z_T) = (20\text{ m}, 4\text{ m}, 0)$, $(x_R, y_R, z_R) = (40\text{ m}, 2\text{ m}, 0)$, $f_c = 5.4$ GHz, $f_{\max} = 100$ Hz, $l = k = 1$, and $l' = k' = 2$. It is stated in [16] that NLoS rays have great influence on the channel characteristics; thus, we assume the average power of NLoS rays equals that of the LoS components (i.e., $C_R = 1$). The energy-related parameter η_i is related to the cases of the reflected numbers of the NLoS scattering paths N. Moreover, we assume N to be even for simplicity and have $\eta_1 = 0.5, \eta_2 = 0.5$ when $N = 2$; $\eta_1 = 0.5$, $\eta_2 = 0.25, \eta_3 = 0.125$, $\eta_4 = 0.125$ when $N = 4$; and $\eta_1 = 0.5, \eta_2 = 0.25, \eta_3 = 0.125$, $\eta_4 = 0.0625$, $\eta_5 = 0.03125, \eta_6 = 0.03125$ when $N = 6$.

First, by using $\rho_{lk,l'k'}(t,\tau) = \rho_{lk,l'k'}^{LOS}(t,\tau) + \rho_{lk,l'k'}^{NLOS}(t,\tau)$, the time-variant space CFs for the proposed ellipsoid scattering model, with respect to the reflection number and the radius of the tunnel, are depicted by Figure 2 when $t = 0s, M_T = M_R = 4, \gamma_T = 2\pi/3$, $\gamma_R = \pi/6, v_R = 54$ km/h, and $\phi_v = \pi/3$. In general, the space CFs gradually decrease when the normalized antenna spacing δ_R/λ increases. A similar behavior can be seen in [13]. Moreover, it can be found that when the proposed channel involves no scattering

(i.e., $N = 0$), the space CFs have no relation with the tunnel parameters. However, note that when the multi-bounced scattering rays are taken into account, the space correlations of the proposed model become much smaller on account of the higher geometric path lengths, which fits with the outcomes in model [8,9], thereby validating the necessity of considering the multi-bounced scattering assumption for our proposed model. In addition, when the reflection number and the radius of the tunnel increase, the correlations reduce correspondingly, as shown in Figure 2.

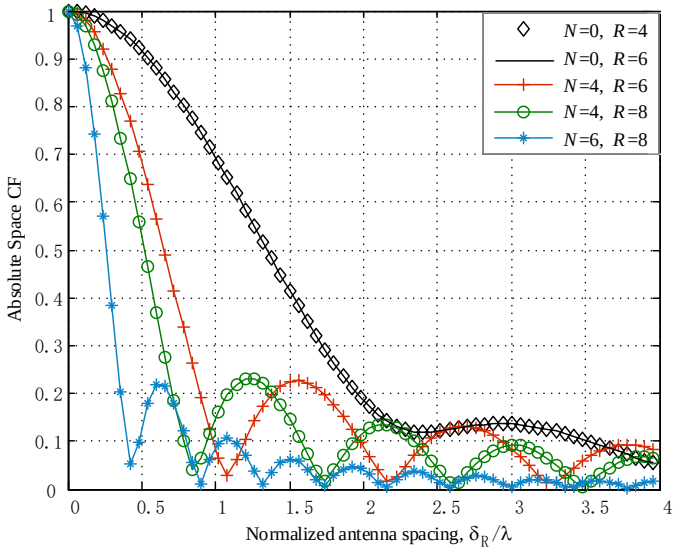

Figure 2. Proposed time-variant space CFs for the LoS and NLoS paths, with respect to the reflection number N and the radius of the tunnel R.

Furthermore, by using Equation (13), Figures 3 and 4 depict the proposed time-variant space CFs for the NLoS paths in the case of different moving properties and numbers of the transmitter and receiver antennas (i.e., M_T and M_R) with different antenna angles, respectively. It can be noticed, in Figure 3, that when the MR moves toward to the MT (i.e., $\phi_v = 0$), the correlation is relatively higher than that when the MR moves back to the MT and perpendicular to the x'-axis (i.e., $\phi_v = \pi$ and $\phi_v = \pi/2$). Furthermore, we can also conclude that when the velocity v_R increases from 50 km/h to 60 km/h, the correlation gradually decreases in the case of the same moving direction. Meanwhile, the distributions of the space CFs match the statistical properties in the Jiang model [10] well, demonstrating the correctness of involving the non-stationarity for the proposed vehicular tunnel channel.

As mentioned in [17,18], the multiple heterogeneous networks are supposed to enable future mobile networks to work in almost every conceivable environment; there will be a variety of multi-band and multi-cell channels to be characterized. Therefore, the traditional antenna array technology has been unable to meet the increasing traffic demands of mobile wireless communication networks. Subsequently, Jiang [10] introduced a massive MIMO antenna array model for future vehicle-to-vehicle communication environments, in which the time and frequency cross-correlation functions for different propagation paths are taken into account. Meanwhile, the measurements in both [10,13] demonstrate that the correlation decreases gradually with the increase of the number of transmitter and receiver antennas, which confirms the results in Figure 4. However, they neglected the impact of the orientations of the transmitter and receiver antenna arrays on the channel characteristics. Further, we can notice from Figure 4 that when the antenna angle γ_R increases, the correlation decreases therewith.

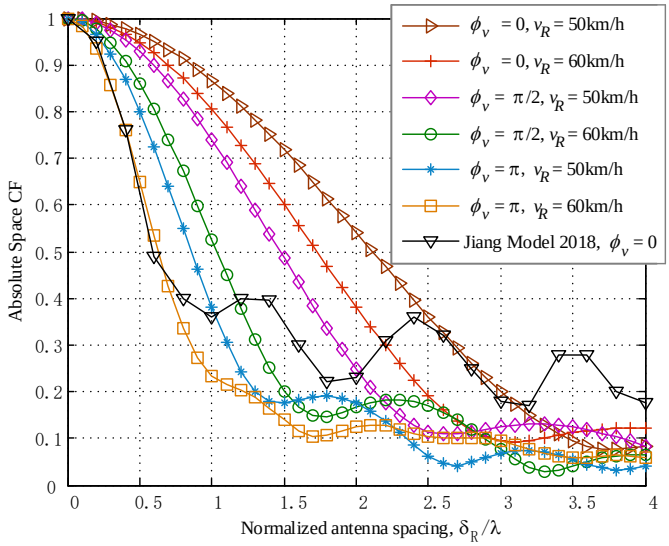

Figure 3. Proposed time-variant space CFs for the NLoS paths in the case of different moving properties ϕ_v and v_R, when $t = 2s, N = 4, R = 6$ m, $M_T = M_R = 4, \gamma_T = 2\pi/3$, $\gamma_R = \pi/6$ [10].

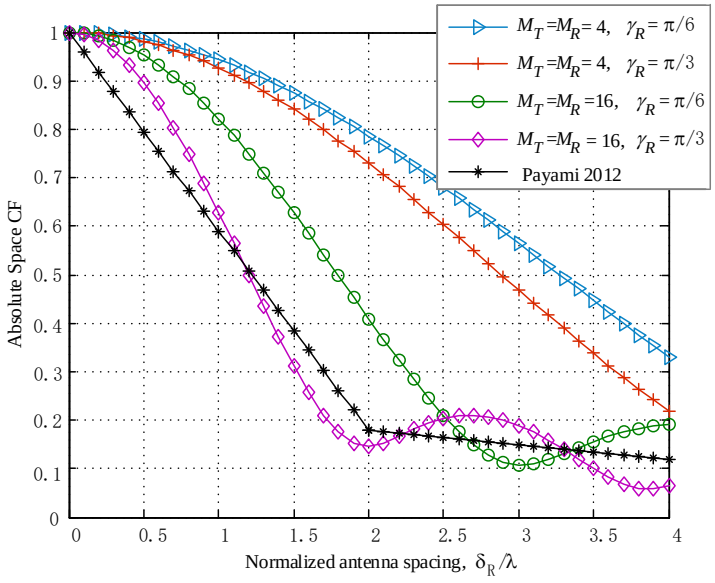

Figure 4. Proposed time-variant space CFs for the NLoS paths, with respect to numbers of the transmitter/receiver antennas and different antenna angles γ_R, when $t = 0$ s, $N = 4$, $R = 6$ m, $\gamma_T = 2\pi/3$, $v_R = 54$ km/h, and $\phi_v = 0$ [13].

Similarly, we can further investigate the proposed time-variant frequency CFs on both the LoS and NLoS propagation rays, as shown in Equation (14), which measures the frequency selectivity of the proposed channel model.

$$\begin{aligned}\rho_{lk,l'k'}(t,\Delta f) = {} & C_R e^{j2\pi[f_{\max}\cos(\phi))t-\Delta f\left(D_{Tk}^{(l,k)}-D_{TR}^{(l,k)}\right)/c]} \\ & + \frac{3\eta_i}{2\pi Rab}\int_{-\pi}^{\pi}\int_{0}^{\pi/2} e^{j2\pi t f_{\max}\cos(\arcsin[(r_b\sin\theta)/r_m]+\phi_v\}} \\ & \times e^{-j2\pi\left(D_T^{(l,m)}+D_R^{(m,k)}-D_T^{(l',k)}-D_R^{(m,k')}\right)\Delta f/c} d\beta d\theta \end{aligned} \quad (14)$$

with c representing the speed of light. Subsequently, if we set $t = 0$, then the frequency correlation function can be derived as

$$\rho(\Delta f) = \frac{3\eta_i}{2\pi Rab}\int_{-\pi}^{\pi}\int_{0}^{\pi/2} e^{-j2\pi\Delta f\left(D_T^{(l,m)}+D_R^{(m,k)}(0)-D_T^{(l',m)}-D_R^{(m,k)}(0)\right\}/c} d\beta d\theta + C_R e^{j2\pi\Delta f\left(D_0^{(l,k)}-D_0^{(l',k)}\right)/c} \quad (15)$$

Figure 5 illustrates the distributions of the proposed frequency CFs in the case of different reflection numbers and radii of the tunnel. It is observed that the frequency correlations is drastically reduced by between 0–5 MHz under different parameter conditions. However, the curves show slight concussions after the frequency of 5 MHz. Meanwhile, when the reflection number and radius of the tunnel increase, the amplitude concussion of the mutual frequency function decreases relatively. In general, the frequency cross-correlations of the proposed reference channel model seem not very sensitive to changes in parameters. Furthermore, the frequency CFs in Figure 5 show similar trends with those of the geometric channel model [4], and perform much better within 40 MHz, illustrating the feasibility of the proposed model for describing tunnel V2V environments.

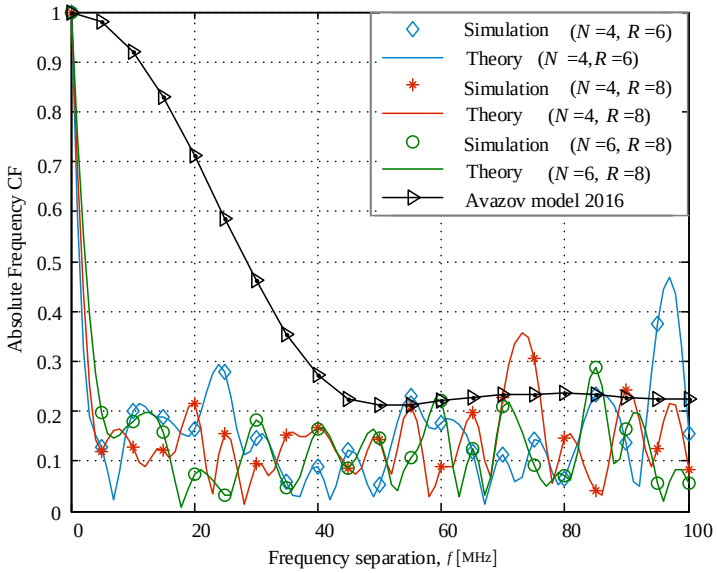

Figure 5. Proposed frequency CFs for the LoS and NLoS paths in terms of the reflection number N and the radius of the tunnel R when $M_T = M_R = 4$, $\gamma_T = 2\pi/3$, $\gamma_R = \pi/6$, $v_R = 54$ km/h, and $\phi_v = pi/3$ [4].

5. Conclusions

In this work, we present a modified geometry-based scattering model for typical tunnel V2V communication environments under an assumption of equivalent scattering points. The effects of tunnel parameters and moving properties on the time-varying channel CFs are further investigated. Numerical results show that when the multi-bounced scattering rays are taken into account, the space correlations of the proposed model become much smaller on account of the higher geometric path lengths; furthermore, when the velocity increases, the correlation gradually decreases in the case of the same moving direction. Moreover, as the antenna angle γ_R increases, the correlation decreases therewith. Comparisons with existing geometric V2V channel models and tunnel measurements verify the utility of the proposed multi-bounced scattering model for tunnel situations. For future work, we would like to perform experiment verification and consider the computation overhead or minor responsiveness in the execution of algorithms.

Author Contributions: Writing—review and editing, supervision, project administration, and funding acquisition: D.T. and X.X. (D.T. and X.X. contributed equally to this work as co-correspondent authors). Methodology, software, writing—original draft preparation: D.T. and Q.F. All authors have read and agreed to the published version of the manuscript.

Funding: The research was supported by the National Nature Science Foundation of China (grant numbers 61771389 and 61701398).

Institutional Review Board Statement: Not applicable.

Informed Consent Statement: Not applicable.

Data Availability Statement: Not applicable.

Conflicts of Interest: The authors declare no conflict of interest.

References

1. Jiang, H.; Zhang, Z.; Wu, L.; Dang, J.; Gui, G. A 3-D non-stationary wideband geometry-based channel model for MIMO vehicle-to-vehicle communications in tunnel environments. *IEEE Trans. Veh. Technol.* **2019**, *68*, 6257–6271. [CrossRef]
2. Arshad, K.; Katsriku, F.; Lasebae, A. Modelling obstructions in straight and curved rectangular tunnels by finite element approach. *J. Electr. Eng.* **2008**, *59*, 9–13.
3. Forooshani, A.E.; Noghanian, S.; Michelson, D.G. Characterization of angular spread in underground tunnels based on the multimode waveguide model. *IEEE Trans. Commun.* **2014**, *62*, 4126–4133. [CrossRef]
4. Avazov, N.; Pätzold, M. A Novel Wideband MIMO Car-to-Car Channel Model Based on a Geometrical Semicircular Tunnel Scattering Model. *IEEE Trans. Veh. Technol.* **2016**, *65*, 1070–1082. [CrossRef]
5. Zhang, J.; Tao, C.; Liu, L. A study on channel modeling in tunnel scenario based on propagation graph theory. In Proceedings of the IEEE 83rd Vehicular Technology Conference (VTC Spring), Nanjing, China, 15–18 May 2016.
6. Ghoraishi, M.; Ching, G.; Lertsirisopon, N. Polar directional characteristics of the urban mobile propagation channel at 2.2 GHz. In Proceedings of the 3rd European Conference on Antennas and Propagation, Berlin, Germany, 23–27 March 2009.
7. Zhou, W.; Pätzold, M.; Chen, W.; He, Z. A simulation model for wideband MIMO vehicle-to-vehicle fading channels in T-junction propagation environments. In Proceedings of the URSI International Symposium on Electromagnetic Theory, Berlin, Germany, 16–19 August 2010.
8. He, D.; Ai, B.; Guan, K.; Zhong, Z.; Hui, B.; Kim, J.; Chung, H.; Kim, L. Stochastic Channel Modeling for Railway Tunnel Scenarios at 25 GHz. *ETRI J.* **2018**, *40*, 39–50. [CrossRef]
9. Tang, D.; Xi, X.; Fan, Q. Analysis of modified multi-bounced scattering channel model for dense tunnel vehicle-to-vehicle communication environment. *Acta Electron. Sinca* **2021**, *49*, 887–893.
10. Jiang, H.; Zhang, Z.; Dang, J.; Wum L. A novel 3D massive MIMO channel model for vehicle-to-vehicle communication environments. *IEEE Trans. Commun.* **2018**, *66*, 79–90. [CrossRef]
11. Jiang, H.; Xiong, B.; Zhang, Z.; Zhang, J.; Zhang, H.; Dang, J.; Wum L. Novel statistical wideband MIMO V2V channel modeling using Unitary matrix transformation algorithm. *IEEE Trans. Wirel. Commun.* **2021**, *20*, 4947–4961. [CrossRef]
12. Jiang, H.; Ruan, C.; Zhang, Z.; Dang, J. Wu, L.; Mukherjee, M.; Benevides, D. A general wideband non-stationary stochastic channel model for intelligent reflecting surface-assisted MIMO communications. *IEEE Trans. Wirel. Commun.* **2021**, *20*, 5314–5328. [CrossRef]
13. Payami, S.; Tufvesson, F. Channel measurements and analysis for very large array systems at 2.6 GHz. In Proceedings of the 6th EUCAP, Prague, Czech Republic, 26–30 March 2012.
14. Yuan, Y.; Wang, C.; Ghazal, A.; Aggoune, E.M.; Alwakeel, M.M. Performance Investigation of Spatial Modulation Systems under Non-Stationary Wideband High-Speed Train Channel Models. *IEEE Trans. Wirel. Commun.* **2016**, *15*, 6163–6173.
15. Zajic, A.G. Impact of moving scatterers on vehicle-to-vehicle narrow-band channel characteristies. *IEEE Trans. Veh. Technol.* **2014**, *63*, 3094–3106. [CrossRef]
16. Jiang, H.; Mukherjee, M.; Zhou, J.; Lloret, J. Channel modeling and characteristics analysis for 6G wireless communications. *IEEE Netw.* **2021**, *35*, 296–303. [CrossRef]
17. Zhang, H.; Yang, L.; Hanzo, L. Compressed Sensing Improves the Performance of Subcarrier Index-Modulation-Assisted OFDM. *IEEE Access* **2016**, *4*, 7859–7873. [CrossRef]
18. Zhang, H.; Hanzo, L. Federated Learning Assisted Multi-UAV Networks. *IEEE Trans. Veh. Technol.* **2020**, *69*, 14104–14109. [CrossRef]